

Nernst effect of epitaxial $\text{Y}_{0.95}\text{Ca}_{0.05}\text{Ba}_2(\text{Cu}_{1-x}\text{Zn}_x)_3\text{O}_y$ and $\text{Y}_{0.9}\text{Ca}_{0.1}\text{Ba}_2\text{Cu}_3\text{O}_y$ films

I. Kokanović^{1,2}, J.R. Cooper¹ and M. Matusiak¹

¹*Department of Physics, University of Cambridge,
J. J. Thomson Avenue, Cambridge CB3 0HE, U.K.*

²*Department of Physics, Faculty of Science, University of Zagreb, P.O.Box 331, Zagreb, Croatia.**

(Dated: November 2, 2018)

We report Nernst effect measurements of some crystalline films grown by pulsed laser deposition, namely slightly under- and nearly optimally-doped $\text{Y}_{0.95}\text{Ca}_{0.05}\text{Ba}_2(\text{Cu}_{1-x}\text{Zn}_x)_3\text{O}_y$ (with $x = 0, 0.02$ and 0.04) and over-doped $\text{Y}_{0.9}\text{Ca}_{0.1}\text{Ba}_2\text{Cu}_3\text{O}_y$. We argue that our results and most of the data for LSCO [1] are consistent with the theory of Gaussian superconducting fluctuations [2].

In conventional type II superconductors, the motion of Abrikosov vortices induced by a thermal gradient ($\nabla_x T$), perpendicular to the magnetic field B , gives rise to a transverse electric field E_y and hence a Nernst voltage, the Nernst coefficient ν being defined by the relation, $\nu = \frac{E_y}{\nabla_x T B}$. In some influential papers, measurements of significant Nernst signals over a broad temperature range *well above* the superconducting transition temperature (T_c) have been reported, initially for $\text{La}_{2-x}\text{Sr}_x\text{CuO}_4$ (LSCO) [1] and later for several other cuprate crystals [3]. These results have been interpreted as evidence for the existence of vortex-like excitations above T_c , and for two separate temperature scales for phase and amplitude fluctuations of the superconducting order parameter. Because ν seemed to be particularly large for under-doped samples, in the pseudogap region of the cuprate phase diagram, it was suggested that the pseudogap is actually caused by superconducting fluctuations, in contradiction to arguments based on heat capacity studies [4]. More recently, by introducing controlled amounts of disorder by electron irradiation [5] or by Zn doping [6] other authors have shown that the onset of a larger Nernst signal is not linked to T^* , the characteristic energy scale of the pseudogap. The Nernst data [1, 3] have also been cited by many authors in support of the scenario in which the pseudogap remains finite over the whole superconducting region of the cuprate phase diagram rather than going to zero for slightly over-doped samples.

Nernst effect studies of the cuprates inspired an extension of the theory of superconducting fluctuations [7] by Ussishkin et al. [2] who showed that for weak (Gaussian) fluctuations (GF), the off-diagonal term, α_{xy}^s , of the Peltier tensor is given by:

$$\alpha_{xy}^s = \frac{k_B e \xi_{ab}^2}{3h l_B^2 s} \frac{1}{\sqrt{1 + (2\xi_c/s)^2}} \quad (1)$$

here ξ_{ab} and ξ_c are the temperature-dependent coherence lengths parallel and perpendicular to the layers, s is the interlayer spacing, $l_B = (\hbar/eB)^{1/2}$ is the magnetic length and the anisotropy $\gamma = \xi_{ab}/\xi_c$. The fluctuation contribution to the Nernst coefficient is given by:

$$\nu_s = \alpha_{xy}^s / [\sigma(T)B] \quad (2)$$

where $\sigma(T)$ is the total electrical conductivity. Ussishkin et al. [2] found that Gaussian superconducting fluctuations account well for Nernst data of optimally doped and over-doped $\text{La}_{2-x}\text{Sr}_x\text{CuO}_4$ crystals with $x = 0.20$ and 0.17 but for an under-doped sample with $x = 0.12$ they suggested that stronger non-Gaussian fluctuations give a larger Nernst signal and also reduce T_c from the mean field value. Recently their GF theory [2] was verified over a wide temperature range by experiments on thin amorphous low-temperature superconductors [8], this is especially important in view of an alternative theoretical viewpoint reported recently [9].

Here we report measurements of the Nernst effect for the same Ca and Zn substituted $\text{YBa}_2\text{Cu}_3\text{O}_{6+x}$ (YBCO) epitaxial films for which in-plane resistivity and magnetoresistivity $\rho(B, T)$, and Hall coefficient R_H , data were previously reported [10]. We show that our Nernst data above T_c are consistent with GF theory [2]. Although the Nernst signal is more clearly visible in our Zn-doped samples, we argue that this is primarily because of their smaller conductivity. In contrast to the suggestion of Refs. 5 and 6, for our samples there is no evidence for the Nernst signal being enhanced by another mechanism such as inhomogeneous superconductivity. We also show that GF can account for the general behavior of Nernst data of LSCO [1] over the whole doping range.

Values of the hole concentration p determined from the room-temperature thermopower, $S(290\text{K})$ [11], are given in Table I together with T_c values and transition widths (FWHM, δT_c , in $d\rho/dT$). Small changes in p have occurred since the previous work and therefore quantities such as $\rho(B, T)$ and R_H were measured again below 120 K. In the Nernst set-up used here the $10 \times 5 \times 1 \text{ mm}^3$ SrTiO_3 substrate was glued between copper and stainless steel posts each holding a heater and a small Cernox thermometer. A sketch of the patterned thin film is shown in the insert to Fig. 1(a). The temperature gradient of 2 or 4 K/cm was applied along the longitudinal direction, B was applied along the c direction of the film (perpendicu-

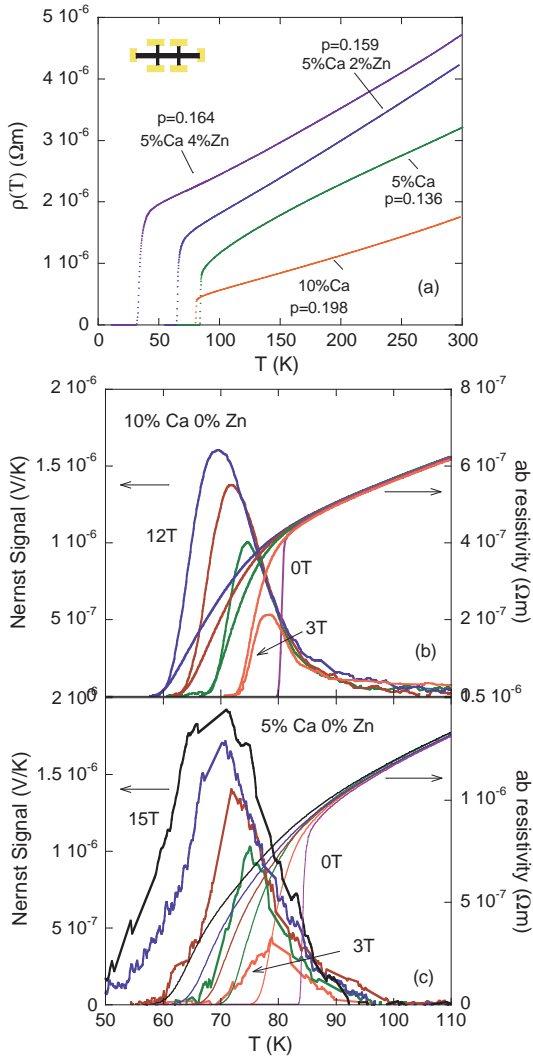


FIG. 1: Color online. (a) In-plane resistivity versus temperature for $\text{Y}_{0.95}\text{Ca}_{0.05}\text{Ba}_2(\text{Cu}_{1-x}\text{Zn}_x)_3\text{O}_y$ ($x = 0, 0.02$ and 0.04) and $\text{Y}_{0.9}\text{Ca}_{0.1}\text{Ba}_2\text{Cu}_3\text{O}_7$ films. (b) Nernst signal versus T at 3, 6, 9 and 12 T for the $\text{Y}_{0.9}\text{Ca}_{0.1}\text{Ba}_2\text{Cu}_3\text{O}_7$ film. (c) Nernst signal versus T at 3, 6, 9, 12 and 15 T for the $\text{Y}_{0.95}\text{Ca}_{0.05}\text{Ba}_2\text{Cu}_3\text{O}_y$ film. In (b) and (c) in-plane resistivities at the same fields and at 0 T are also shown.

lar to the surface of the substrate) and the Nernst signal was measured between the “Hall contacts” using a Keithley Model 182 nanovoltmeter. The transverse voltage V_B was measured for $+B$ and $-B$ while sweeping either T or B , the Nernst voltage was defined as $\frac{1}{2}(V_B - V_{-B})$ and converted to electric field using the distance (1.5 mm) between the inside edges of opposite gold contact pads. ∇T was checked by measuring the thermoelectric voltage between two longitudinal contacts. The precise temperature of the sample was determined by comparing $\rho(T, B)$ data measured with and without an applied temperature gradient.

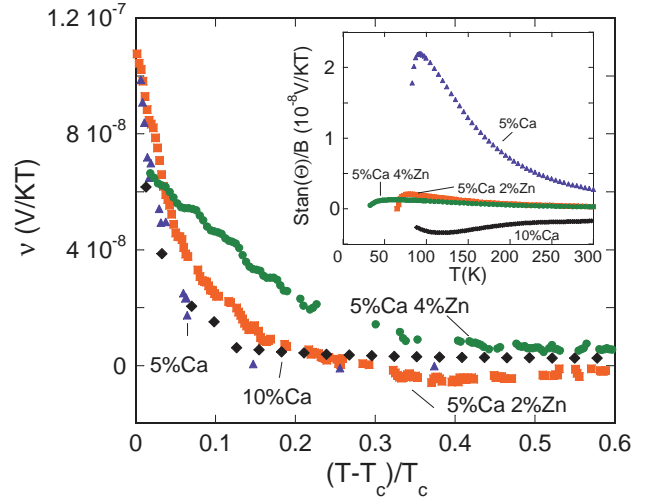


FIG. 2: Color online: Nernst coefficient, ν , versus reduced temperature t for the $\text{Y}_{1-z}\text{Ca}_z\text{Ba}_2(\text{Cu}_{1-x}\text{Zn}_x)_3\text{O}_y$ ($z = 0.05, 0.1$; $x = 0, 0.02$ and 0.04) films. Inset shows $S \tan(\theta)/B$, where S is the thermopower and θ the Hall angle in a field $B = 6\text{T}$.

Zero-field $\rho(T)$ data for the four films are shown in Fig. 1(a). Representative $\rho(T, B)$ and Nernst data are shown for the over-doped 10 % Ca sample ($p = 0.198$) in Fig. 1(b) and for the most under-doped 5 % Ca sample ($p = 0.136$) in Fig. 1(c). The $\rho(T, B)$ curves show the usual “fanning out” property which is typical of the cuprates but is not observed in conventional type II superconductors. The points at which $\rho(T, B) \simeq 0$ on the scales shown correspond to the irreversibility line $B_{irr}(T)$. Many researchers consider that for $B > B_{irr}(T)$ there is a wide “vortex liquid” region where vortices are still present but no longer form a regular lattice and are no longer pinned. We have argued previously [12, 13] for an alternative viewpoint in which the vortices disappear for B equal to, or slightly greater than, $B_{irr}(T)$. In other words $B_{irr}(T)$ could actually be the $B_{c2}(T)$ line which has been heavily suppressed by superconducting fluctuations that may be further enhanced by the magnetic field. This view is still controversial but is not inconsistent with a recent dynamical scaling analysis of voltage-current measurements for YBCO single crystals and films [14].

If one does assume that vortices are still present well above $B_{irr}(T)$ then the ratio $\nu(T, B)/\rho(T, B)$ can be used to determine the entropy per vortex as has been done for LSCO [15]. This assumes isotropic vortex pinning forces, since the resistivity arises from sideways motion of the vortices (perpendicular to the direction of current flow) while the Nernst voltage arises from the flow of vortices along the length of the sample. In Fig. 1(b) the onset of the Nernst signal is the same as the onset of resistivity to within experimental uncertainty of ± 0.5

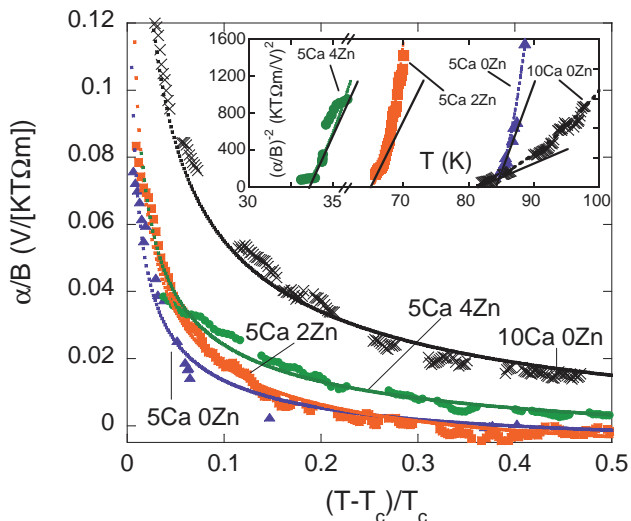


FIG. 3: Color online: $\alpha/B \equiv \sigma_{ab}(T)\nu$ versus t for $Y_{0.95}Ca_{0.05}Ba_2(Cu_{1-x}Zn_x)_3O_y$ ($x = 0, 0.02, 0.04$) and $Y_{0.9}Ca_{0.1}Ba_2Cu_3O_y$ films. The thin dotted lines show fits to Eq. 1. The inserts are plots of $(\alpha/B)^{-2}$ versus T near T_c , with dashed lines showing the fits to Eq. 1 and solid lines the linear 3D limit of Eq. 1.

K while data for the under-doped 5 % Ca sample in Fig. 1(c) show sizeable Nernst signals ~ 6 K below the points at which $\rho(T, B) = 0$. Vortex pinning at twin boundaries is known to be important in YBCO based compounds and can be highly anisotropic [16]. We therefore believe that the different behavior of the two samples is not directly linked to their different doping levels, but arises because anisotropic pinning by twin boundaries is significant for the data in Fig. 1(c) but not for those in Fig. 1(b).

Figure 2 shows the Nernst coefficient above T_c for all four samples *vs.* the reduced temperature $t \equiv (T - T_c)/T_c$ up to $t = 0.6$. Here the initial linear part of the Nernst voltage versus B curve has been used to determine ν . As T_c is approached from above, these curves become non-linear at a field of 1-2 $\times (T - T_c)$ Tesla. This is to be expected for GF which are gradually suppressed when l_B becomes comparable with $\xi_{ab}(T)$, or equivalently when $B \sim (T - T_c) |dB_{c2}/dT|$ where dB_{c2}/dT is the slope of B_{c2} just below T_c and is 1-2 T/K for cuprates with T_c values of 80 to 90 K. The criterion used in Ref. 1 for a significant ‘‘vortex’’ signal is $\nu = 4$ nV/K-Tesla. At first sight this might suggest that there are vortices up to $t \simeq 0.6$ in our 4 % Zn doped sample, and that disorder increases the temperature difference between the formation of fluctuating Cooper pairs and the onset of phase coherence, as proposed for electron-irradiated YBCO samples [5]. However we reject this hypothesis and argue below that the observed value of ν arises simply from GF. One reason for the apparent enhancement of ν is that any normal state (quasiparticle) contribution ν_n is suppressed by Zn doping. $|\nu_n|$ is expected

TABLE I: Summary of results

Sample <i>Ca, Zn</i>	T_c (K)	δT_c (K)	p (holes/Cu)	ξ_{ab} (nm)	γ
0.05	84.2	0.6	0.136 ± 0.002	1.6 ± 0.2	6.2 ± 0.5
0.05, 0.02	65.1	1	0.159 ± 0.004	1.9 ± 0.2	7.2 ± 0.5
0.05, 0.04	33.3	1.5	0.164 ± 0.004	2.6 ± 0.2	5.1 ± 0.5
0.1	80.6	0.7	0.198 ± 0.004	3.4 ± 0.2	7.5 ± 0.5

to be smaller than $|S \tan \theta_H|$ where S is the thermoelectric power and θ_H the Hall angle in the normal state, given by $\tan \theta_H \equiv \sigma_{xy}/\sigma_{xx} = \rho_{xy}/\rho_{xx}$. The condition $|\nu_n| \ll |S \tan \theta_H|$ arises from the Sondheimer cancellation [17] between the off-diagonal thermal and electrical currents that is exact for a single parabolic band with an energy independent relaxation time [18]. If these rather restrictive conditions do not apply, then we expect that $|\nu_n| \sim |S \tan \theta_H|$. As shown in the inset to Fig. 2, for the two Zn doped films, $S \tan \theta_H$ is particularly small which makes the GF term more visible.

Fig. 3 shows $\alpha/B \equiv \sigma_{ab}(T)\nu$ vs. t for the same samples as in Fig. 2 together with fits to Eq. 1 with $s = 1.17$ nm, the c -axis lattice parameter. An extra fitting parameter, a small offset $\simeq -0.01$ V/K-T- Ω m, has been included in Eq. 1 to account for ν_n . In the 3D limit of Eq. 1 near T_c where $\xi_c(T) \gg s$, we expect $\alpha^{-2} \propto (T - T_c)$. Corresponding plots are shown in the insert to Fig. 3. There are small linear regions extrapolating to $y = 0$ near the measured value of T_c . At higher T these cross over to the quadratic law, $\alpha^{-2} \propto (T - T_c)^2$ expected in the 2D limit. A similar analysis [19] of the heat capacity of several cuprate families showed that the difference, ΔT_c , between the measured value, T_c^m , and the fitted or linearly extrapolated value, T_c^f , was caused by strong (critical) fluctuations. ΔT_c was ~ 1 K for YBCO samples, as found for the present Nernst data, and ~ 5 K for other extremely anisotropic cuprates.

The fitting parameters $\xi_{ab}(T = 0)$ and $\gamma \equiv \xi_{ab}/\xi_c$ are summarized in Table I. The value $\xi_{ab}(0) = 1.6$ nm for the 5 % Ca sample corresponds to $B_{c2}(0) \equiv \Phi_0/2\pi\xi_{ab}(0)^2 = 130$ T for $B \parallel c$ and also agrees with the value obtained by GF analysis of heat capacity data [19]. The value of γ also agrees with other estimates for well-oxygenated YBCO [13]. The values of $\xi_{ab}(0)$ for the two Zn-doped films are larger. For the 2 % Zn film, $1/\xi_{ab}(0)$ scales with T_c as expected, but for the 4 % Zn film the short mean free path probably reduces $\xi_{ab}(0)$ according to the standard dirty-limit formula [20]. The coherence length of the 10 % Ca, 0 % Zn film is longer than that for the 5 % Ca, 0 % Zn film. This is not understood, however $\rho(T)$ is a factor of 2 smaller, and also for 10 % Ca, Eq. 1 gives a good fit with $\xi_{ab}(0) = 2.2$ nm and $\gamma = 12$ over a smaller range of t (between 0.03 and 0.2).

The success of the GF analysis described above encouraged us to look again at published data for LSCO

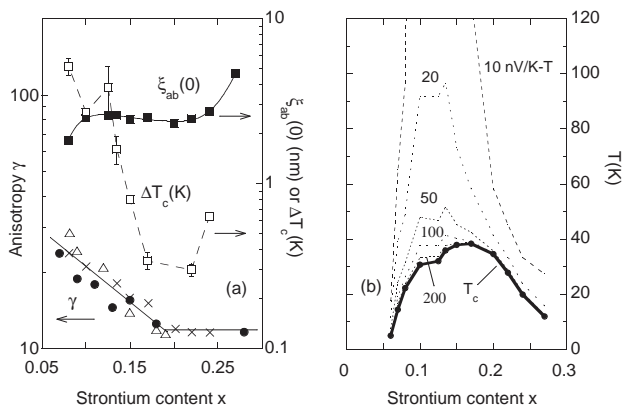


FIG. 4: (a) Left hand scale, anisotropy, $\gamma \equiv \xi_{ab}(0)/\xi_c(0)$, obtained from the room temperature resistivity anisotropy [23] (\bullet) and two sets of London penetration depth data at low T (\times) [21] and (Δ) [22], vs Sr content x in LSCO. Straight lines show average values of γ used in calculations. Right hand scale, $\xi_{ab}(0)$ obtained from a GF analysis [19, 25] of heat capacity (C_v) data [4] above T_c using the same values of γ . $\Delta T_c(x)$ [25] is related to the strength of critical (non-Gaussian) fluctuations [19]. (b) Calculated constant ν contours in the (T, x) plane, using Eqs. 1 and 2, with $s = 0.66$ nm, $\rho_{ab}(x, T)$ from Ref. 24 and $\xi_{ab}(0)$ and γ from Fig. 4(a).

crystals, since Fig. 4 of Ref. [1] and other versions [3, 18] provide key support for the alternative, widely accepted, phase fluctuation and pseudogap pictures. In Fig. 4(a) we show values of γ obtained from the anisotropy in the London penetration depth at low T [21, 22] and from that in $\rho(300K)$ [23] as well as values of $\xi_{ab}(0)$ obtained from GF analysis [19] of the electronic specific heat [4] above T_c . These have been used in Eqs. 1 and 2, together with the measured values of $T_c(x)$ [4] and $\rho_{ab}(T, x)$ [23, 24], to calculate the contour plots for ν shown in Fig. 4(b). This GF picture correctly accounts for the peaked structure of ν vs. Sr content (x) and the magnitude of ν between 40 and 80 K [1, 3, 18]. The asymmetric GF peak arises from the dome-shaped $T_c(x)$ curve and the approximately linear increase of $\sigma_{ab}(T)$ with x [23, 24]. Above 80 K GF theory gives values of ν which are too large, possibly because the fluctuations are suppressed by inelastic scattering processes. In the experimental contour plot [1], there is a small region, $x \leq 0.13$ and $T - T_c \leq 5$ K, where $\nu \simeq 500$ nV/K-T is too large to be consistent with GF theory. Fig. 4(a) shows that $\Delta T_c \sim 2 - 5$ K for $x \leq 0.13$, supporting the idea [2] that in this small region ν is enhanced by critical (non-Gaussian) fluctuations.

In summary we find that weak (Gaussian) superconducting fluctuations account for our Nernst data for YBCO ab-plane films substituted with various levels of Ca and Zn, until at least 30 K above T_c . They also account for the main features of the Nernst contour plots for LSCO crystals.

We are grateful to J. W. Loram and S. H. Naqib for fruitful collaboration and many useful suggestions.

This work was supported by EPSRC (UK), grant number EP/C511778/1 and the Croatian Research Council, MZOS project No. 119-1191458-1008.

* Electronic address: kivan@phy.hr

- [1] Z. A. Xu, N. P. Ong, Y. Wang, T. Kakeshita, and S. Uchida, *Nature (London)* **406**, 486 (2000).
- [2] I. Ussishkin, S. L. Sondhi, and D. A. Huse, *Phys. Rev. Lett.* **89**, 287001 (2002).
- [3] Y. Wang, L. Li and N. P. Ong, *Phys. Rev. B* **73**, 024510 (2006).
- [4] J. W. Loram, J. Luo, J. R. Cooper, W. Y. Liang and J. L. Tallon, *J. Phys. Chem. Sol.* **62**, 59 (2001).
- [5] F. Rullier-Albenque, R. Tourbot, H. Alloul, P. Lejay, D. Colson, and A. Forget, *Phys. Rev. Lett.* **96**, 067002 (2006).
- [6] Z. A. Xu, J. Q. Shen, S. R. Zhao, Y. J. Zhang, and C. K. Ong, *Phys. Rev. B* **72**, 144527 (2005).
- [7] A. Larkin and A. Varlamov, "Theory of Fluctuations in Superconductors", Clarendon Press, Oxford (U.K.) (2005).
- [8] A. Pourret, H. Aubin, J. Lesueur, C. A. Marrache-Kikuchi, L. Bergé, L. Dumoulin, and K. Behnia, *Nature Physics*, **2**, 683 (2006).
- [9] A. Sergeev, M. Y. Reizer and V. Mitin, arXiv0708.1003v1 [cond-mat.supr-con] (2007), to appear in *Phys. Rev. B*.
- [10] I. Kokanović, J. R. Cooper, S. H. Naqib, R. S. Islam and R. A. Chakalov, *Phys. Rev. B* **73**, 184509 (2006).
- [11] S. D. Obertelli, J. R. Cooper, and J. L. Tallon, *Phys. Rev. B* **46**, 14928 (1992).
- [12] J. R. Cooper, J. W. Loram, J. D. Johnson, J. W. Hodby, and C. Changkang, *Phys. Rev. Lett.* **79**, 1730 (1997).
- [13] D. Babić, J. R. Cooper, J. W. Hodby, and C. Changkang, *Phys. Rev. B* **60**, 698 (1999).
- [14] S. Li, H. Xu, S. M. Anlage, M. C. Sullivan, K. Segawa, Y. Ando, and C. J. Lobb, arXiv0803.0961v1[cond-mat.supr-con](2008).
- [15] C. Capan, *et al.*, *Phys. Rev. Lett.* **88**, 056601 (2002).
- [16] S. Fleshler, *et al.*, *Phys. Rev. B* **47**, 14448 (1993).
- [17] H. Sondheimer, *Proc. R. Soc. London, Ser. A* **193**, 484 (1948).
- [18] Y. Wang, *et al.*, *Phys. Rev. B* **64**, 224519 (2001).
- [19] J. W. Loram, J. R. Cooper, J. M. Wheatley, K. A. Mirza and R. S. Liu, *Phil. Mag.* **65**, 1405, (1992).
- [20] J. R. Waldram, "Superconductivity of Metals and Cuprates" (IOP, Bristol, 1996) Chap. 10.
- [21] C. Panagopoulos, T. Xiang, W. Anukool, J. R. Cooper, Y. S. Wang and C. W. Chu, *Phys. Rev. B* **67**, 220502(R) (2003).
- [22] T. Shibauchi, H. Kitano, K. Uchinokura, A. Maeda, T. Kimura, and K. Kishio, *Phys. Rev. Lett.* **72**, 2263 (1994).
- [23] T. Kimura, *et al.*, *Phys. Rev. B* **53**, 8733 (1996).
- [24] Y. Ando, S. Komiya, K. Segawa, S. Ono and Y. Kurita, *Phys. Rev. Lett.* **93**, 267001 (2004).
- [25] Data for the electronic heat capacity, C_v , of LSCO [4] were fitted to the GF expression (Eq. 1 of Ref. 19) plus a linear background. Here $\Delta T_c \equiv T_c^m - T_c^f$, where T_c^m is the midpoint of the step in C_v/T and T_c^f is obtained from the GF fits.